symmetry

MDPI

*Article*

# Symmetric Oscillator: Special Features, Realization, and Combination Synchronization

**Victor Kamdoum Tamba [1], Janarthanan Ramadoss [2], Viet-Thanh Pham [3,4,*], Giuseppe Grassi [5], Othman Abdullah Almatroud [6] and Iqtadar Hussain [7]**

1 Department of Telecommunication and Network Engineering, Fotso Victor University Institute of Technology, University of Dschang, Bandjoun P.O. Box 134, Cameroon; victorkamdoum@yahoo.fr
2 Centre for Artificial Intelligence, Chennai Institute of Technology, Chennai 600069, India; janarthananr@citchennai.net
3 Nonlinear Systems and Applications, Faculty of Electrical and Electronics Engineering, Ton Duc Thang University, Ho Chi Minh City 758307, Vietnam
4 Department of Computer Science and Information Engineering, Asia University, Taichung 41354, Taiwan
5 Dipartimento Ingegneria Innovazione, Universita del Salento, 73100 Lecce, Italy; giuseppe.grassi@unisalento.it
6 Department of Mathematics, Faculty of Science, University of Hai'l, Hai'l 81451, Saudi Arabia; o.almatroud@uoh.edu.sa
7 Mathematics Program, Department of Mathematics, Statistics and Physics, College of Arts and Sciences, Qatar University, Doha 2713, Qatar; iqtadarqau@gmail.com
* Correspondence: phamvietthanh@tdtu.edu.vn

**Abstract:** Researchers have recently paid significant attention to special chaotic systems. In this work, we introduce an oscillator with different special features. In addition, the oscillator is symmetrical. The features and oscillator dynamics are discovered through different tools of nonlinear dynamics. An electronic circuit is designed to mimic the oscillator's dynamics. Moreover, the combined synchronization of two drives and one response oscillator is reported. Numerical examples illustrate the correction of our approach.

**Keywords:** chaos; symmetry; synchronization; circuit



**Citation:** Tamba, V.K.; Ramadoss, J.; Pham, V.-T.; Grassi, G.; Almatroud, A.O.; Hussain, I. Symmetric Oscillator: Special Features, Realization, and Combination Synchronization. *Symmetry* **2021**, *13*, 2142. https://doi.org/10.3390/sym13112142

Academic Editor: Ioan Raşa

Received: 8 October 2021
Accepted: 19 October 2021
Published: 10 November 2021



## 1. Introduction

Several studies have provided important results on chaos [1–3]. Chaos was observed in a memristive system [4], glucose–insulin regulatory system [5], financial system [6], and modified logistic map [7], etc. Panahi et al. proposed a chaotic network model for epilepsy [8], while a chaotic model for HIV virus was introduced in [9]. Chaos is useful for developing applications [10,11]. Potential applications of chaos were reported in wireless communication [12], robot motion [13], authenticated Hash function [14], and pseudo-random generators [15]. Adeyemi et al. introduced the FPGA realization of chaos-encrypted transmission via the parameter-switching technique [16]. Muhammad and Ozkaynak combined chaos, optimization algorithms and physical unclonable functions to design the novel image encryption [17]. Many studies focused on random number generators [18–20]. Moreover, Tutueva et al. improved the random number generators [21].

More recent attention has been concentrated on chaos in systems with special features [22]. Some noticeable features are the absence of linear terms, appearance of many equilibrium points, and multistability. Most studies in the field of chaotic systems have been focused on systems with linear terms. However, results based upon systems without linear terms are limited. Xu and Wang were mentioned that there was much less information about chaotic attractors without a linear term [23]. Therefore, the authors constructed a system with natural logarithmic, exponential and quadratic terms. Using six quadratic terms, a system with eight equilibrium points was proposed in [24]. Zhang et al.

applied a fractional derivative to obtain a new system with six quadratic terms [25]. The authors found four equilibrium points and twin symmetric attractors in Zhang's system. Previously published studies on nonlinear systems paid particular attention to saddle point equilibrium in [26]. The existence of saddle point equilibrium is critical to the design of chaotic systems [27]. Relatively recent research has been found, concerned with different equilibia [28,29]. Recently, investigators have examined chaos in systems with infinite equilibrium [30,31]. Another special feature observed in nonlinear systems is multistability [32]. Depending on the initial conditions, coexisting attractors can be seen. Multistability has emerged as a powerful approach for investigating asymmetric and symmetric attractors [33–35]. Interestingly, multiple attractors attract new research on memristor circuits [36,37].

In this paper, we study a oscillator with nonlinear terms (quadratic and cubic ones). In contrast with conventional systems, there are infinite equilibria in our oscillator. The features and dynamics of the oscillator are presented in Section 2. Section 3 discusses the oscillator's implementation. A combination synchronization of the oscillator is reported in Section 4, while conclusions are provided in the last section.

## 2. Features and Dynamics of the Oscillator

We consider an oscillator described by

$$\begin{cases} \dot{x} = yz \\ \dot{y} = x^3 - y^3 \\ \dot{z} = ax^2 + by^2 - cxy \end{cases} \tag{1}$$

with parameters $a, b, c > 0$. By solving the following equations:

$$\begin{cases} yz = 0 \\ x^3 - y^3 = 0 \\ ax^2 + by^2 - cxy = 0 \end{cases} \tag{2}$$

we get the equilibrium points of oscillator (1):

$$E^*(0, 0, z^*) \tag{3}$$

Therefore, oscillator (1) has an equilibrium line. Oscillator (1) is invariant under the transformation

$$(x, y, z) \to (-x, -y, z) \tag{4}$$

and oscillator (1) is symmetric. Note that the Jacobian matrix at $E^*$ is

$$J_{E^*} = \begin{bmatrix} 0 & z^* & 0 \\ 0 & 0 & 0 \\ 0 & 0 & 0 \end{bmatrix} \tag{5}$$

Therefore, the characteristic equation is $\lambda^3 = 0$ and the eigenvalue $\lambda = 0$.

We fix $a = 0.2$, $b = 0.1$ and the initial conditions $(0.1, 0.1, 0.1)$ while $c$ is varied. The Lypunov exponents (Figure 1a) and bifurcation diagram (Figure 1b) for $c$ are presented. As seen from Figure 1, the oscillator can generate periodical signals and chaotic signals. For $c = 0.5$, chaotic attractors are displayed in Figure 2. We used the Runge–Kutta method for simulations and the Wolf's algorithm for Lypunov exponent calculations [38]. Interestingly, the oscillator displays symmetric attractors, as illustrated in Figure 3. Symmetric attractors coexist with the same parameters ($a = 0.2$, $b = 0.1$, $c = 0.68$) but under different initial conditions. This means that there is multistability in the oscillator. When varying $c$, multistability is reported in Figure 4.

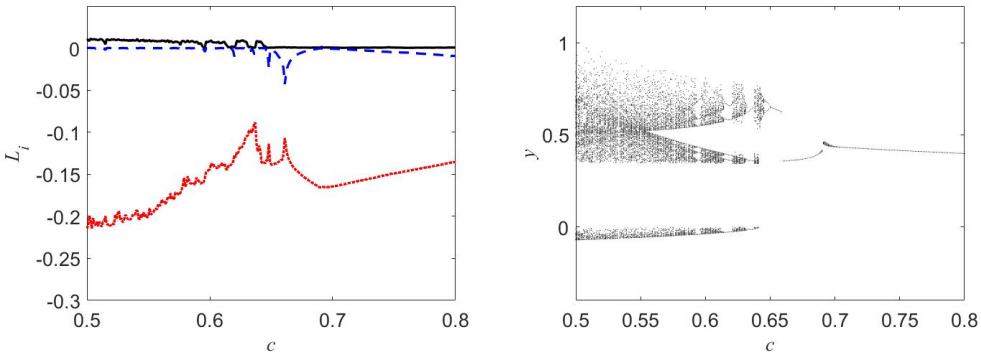


(**a**) (**b**)

**Figure 1.** (**a**) Lypunov exponents; (**b**) Bifurcation diagram of oscillator (1).

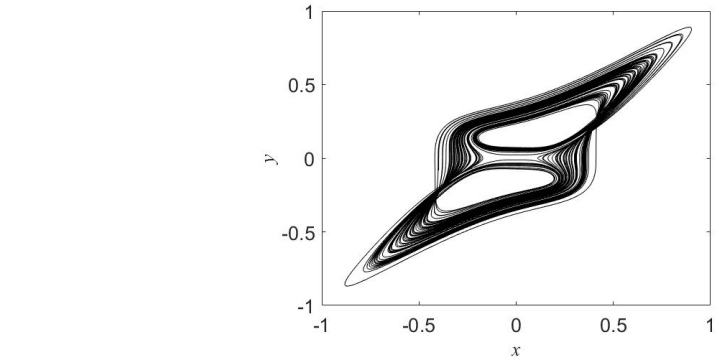


(**a**)

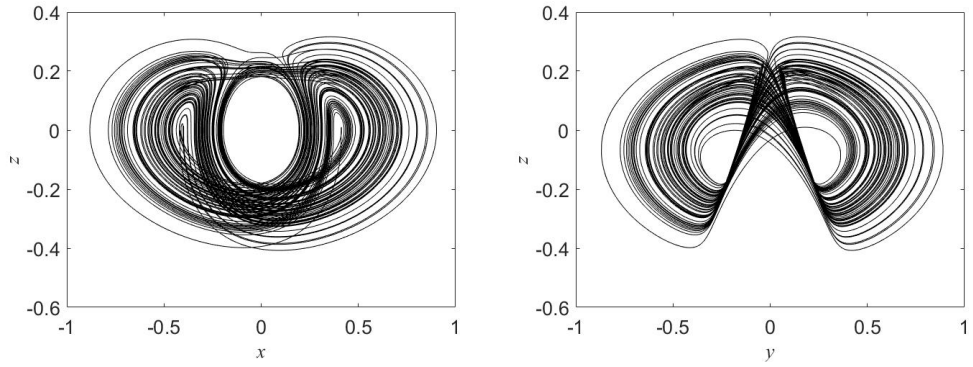


(**b**) (**c**)

**Figure 2.** Chaos in oscillator (1) for $c = 0.5$ in planes (**a**) $x - y$, (**b**) $x - z$, (**c**) $y - z$.

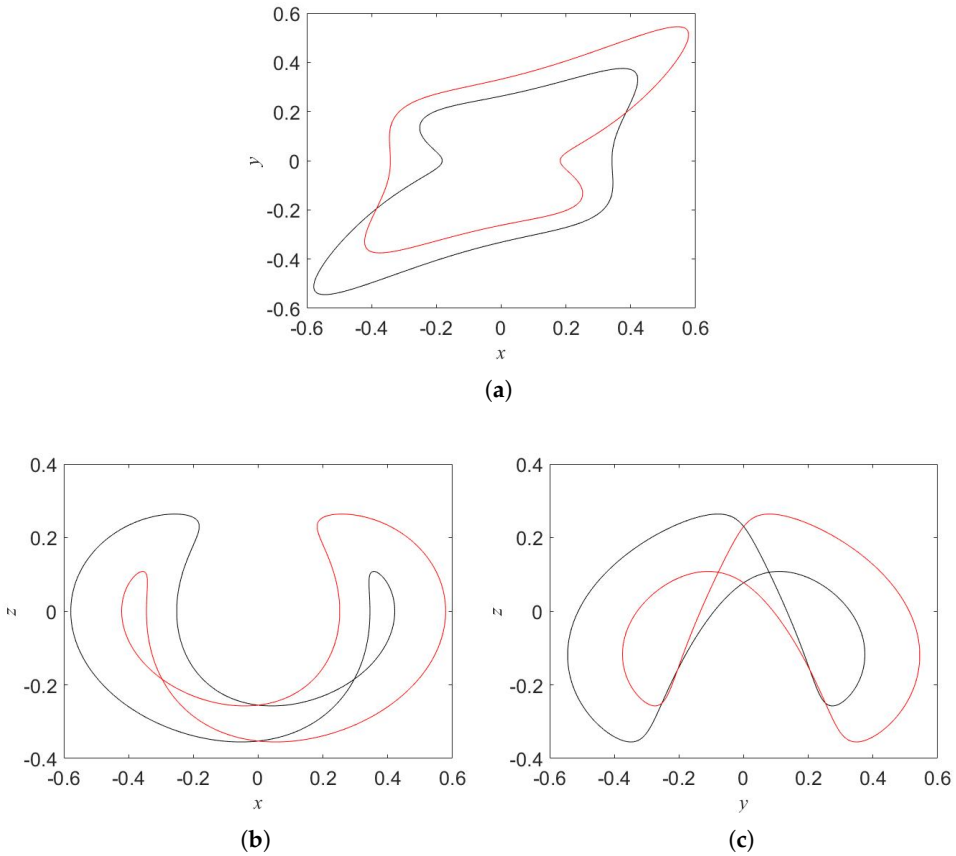


**Figure 3.** Coexisting attractors in the oscillator for $c = 0.68$, initial conditions: $(0.1, 0.1, 0.1)$ (black color), $(-0.1, -0.1, 0.1)$ (red color) in planes (**a**) $x - y$, (**b**) $x - z$, (**c**) $y - z$.

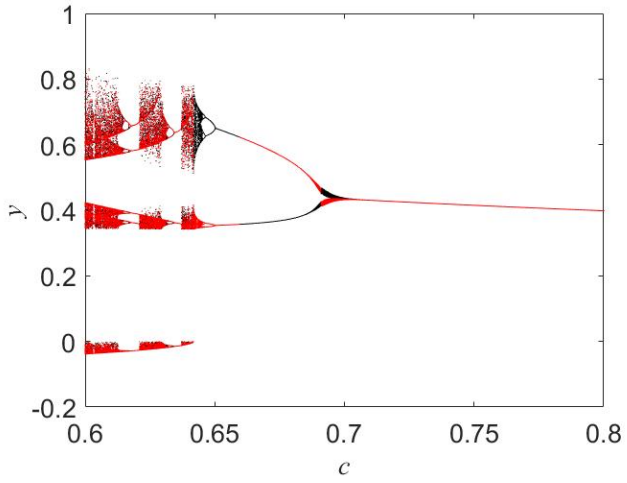


**Figure 4.** Coexisting bifurcation diagrams. Two initial conditions are $(0.1, 0.1, 0.1)$ (black color), $(-0.1, -0.1, 0.1)$ (red color).

Oscillator (1) displays offset boosting dynamics because of the presence of $z$. Consequently, the amplitude of $z$ is controlled by adding a constant $k$ in oscillator (1), which becomes

$$\begin{cases} \dot{x} = y(k+z) \\ \dot{y} = x^3 - y^3 \\ \dot{z} = ax^2 + by^2 - cxy \end{cases} \tag{6}$$

The bifurcation diagram and phase portraits of system (6) in planes $(z-x)$ and $(z-y)$ with respect to parameter $c$ and some specific values of constant parameter $k$ are provided in Figure 5 for $a = 0.2$, $b = 0.1$, $c = 0.5$.

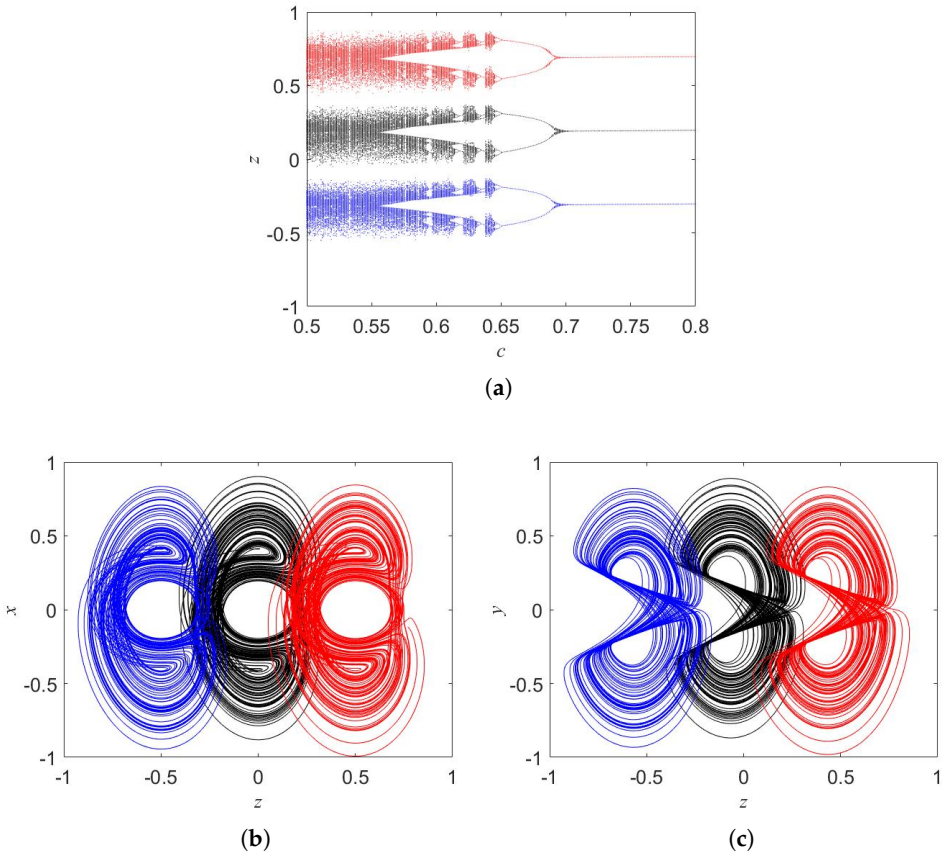


**Figure 5.** (**a**) Bifurcation diagram; (**b**,**c**) Phase portraits of system (6) with respect to $c$ and specific values of constant $k$ illustrating the phenomenon of offset boosting control. The colors for $k = 0, 0.5, -0.5$ are black, blue, and red, respectively. The initial conditions are $(0.1, 0.1, 0.1)$.

From Figure 5, we observe that the amplitude of $z$ is easily controlled through the constant parameter $k$. This phenomenon of offset boosting control has been reported in some other systems [39,40].

## 3. Oscillator Implementation

The electronic circuit of mathematical models displaying chaotic behavior can be realized using basic modules of addition, subtraction, and integration. The electronic circuit implementation of such models is very useful in some engineering applications. The objective of this section is to design a circuit for oscillator (1). The proposed electronic circuit diagram for a system oscillator (1) is provided in Figure 6.

By denoting the voltage across the capacitor $V_v$, $V_y$ and $V_z$, the circuit state equations are as follows:

$$\begin{cases} \frac{dV_x}{dt} = \frac{1}{10R_1C} V_y V_z \\ \frac{dV_y}{dt} = \frac{1}{100R_2C} V_x^3 - \frac{1}{100R_3C} V_y^3 \\ \frac{dV_z}{dt} = \frac{1}{10R_aC} V_x^2 + \frac{1}{10R_bC} V_y^2 - \frac{1}{10R_cC} V_x V_y \end{cases} \tag{7}$$

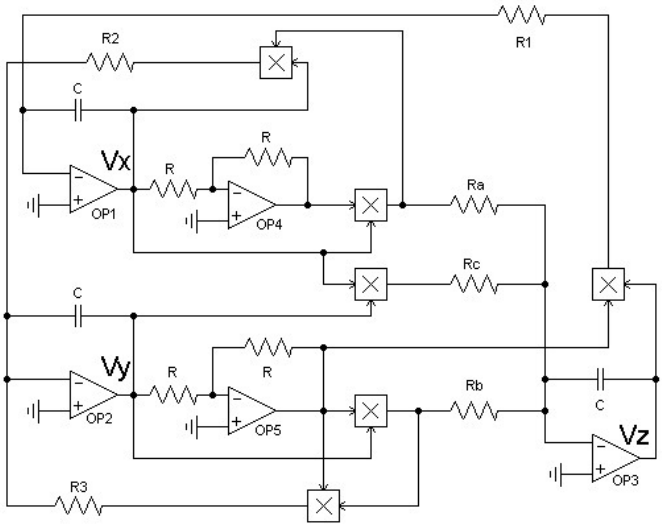


**Figure 6.** Electronic circuit diagram of oscillator (1). It includes operational amplifiers, analog multiplier chips (AD 633JN) that are used to realize the nonlinear terms, three capacitors and ten resistors.

For the system oscillator parameters (1) $a = 0.2$, $b = 0.1$, $c = 0.5$ and initial voltages of capacitor $(V_x, V_y, V_z)$ = $(0.1\text{ V}, 0.1\text{ V}, 0.1\text{ V})$, the circuit elements are $C = 10$ nF, $R_1 = 1$ kΩ, $R_2 = R_3 = 100$ Ω, $R_a = 5$ kΩ, $R_b = 10$ kΩ, and , $R_c = 2$ kΩ. The chaotic attractors of the circuit implemented in PSpice are shown in Figure 7. Moreover, the symmetric attractors of the circuit are reported in Figure 8. As seen from Figures 7 and 8, the circuit displays the dynamical behaviors of special oscillator (1). The real oscillator is also implemented, and the measurements are captured (see Figure 9).

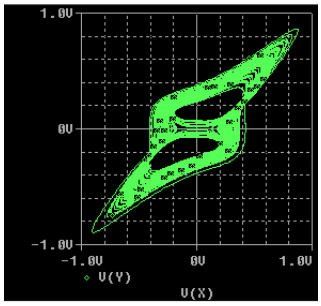


(**a**)

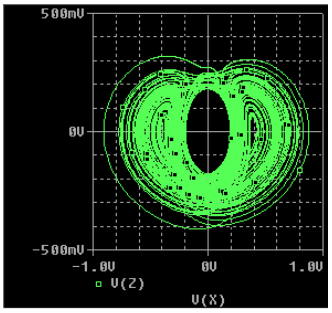


(**b**)

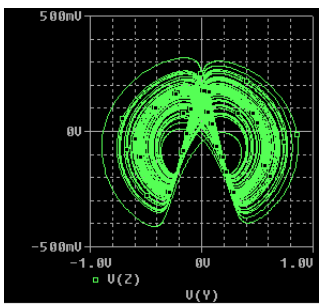


(**c**)

**Figure 7.** Chaotic attractors obtained from the implementation of the PSpice circuit in different planes (**a**) $(V_x, V_y)$, (**b**) $(V_x, V_z)$, and (**c**) $(V_y, V_z)$, for $C = 10$ nF, $R_1 = 1$ kΩ, $R_2 = R_3 = 100$ Ω, $R_a = 5$ kΩ, $R_b = 10$ kΩ, and $R_c = 2$ kΩ. The initial voltages of capacitors are $(V_x, V_y, V_z)$ = $(0.1\text{ V}, 0.1\text{ V}, 0.1\text{ V})$.

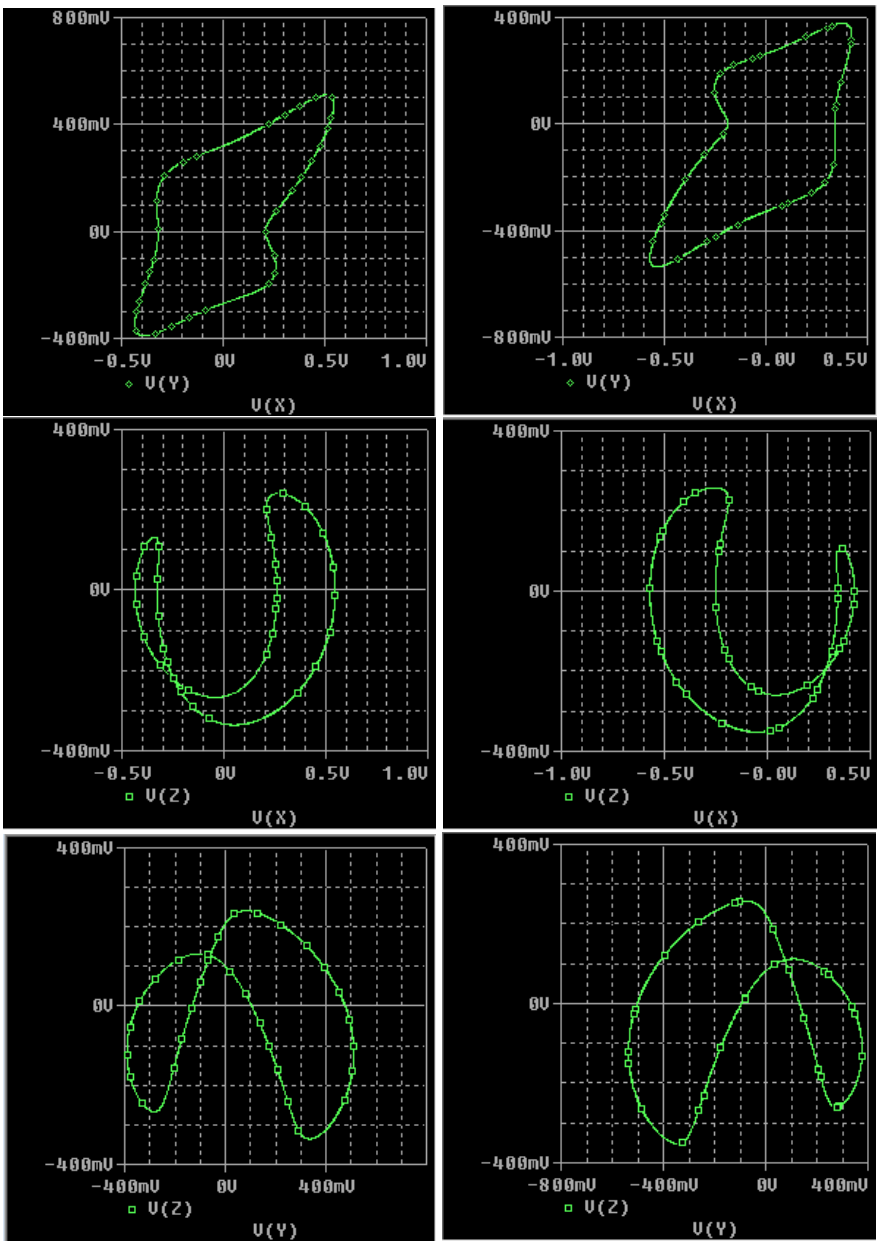


**Figure 8.** Symmetric attractors obtained from the implementation of the circuit in Pspice in different planes $((V_x, V_y)$, $(V_x, V_z)$, $(V_y, V_z))$ for $C = 10$ nF, $R_1 = 1$ kΩ, $R_2 = R_3 = 100$ Ω, $R_a = 5$ kΩ, $R_b = 10$ kΩ, and $R_c = 1.47$ kΩ. The initial voltages of capacitors are $(V_x, V_y, V_z) = (0.1\text{ V}, 0.1\text{ V}, 0.1\text{ V})$ for the left panel and $(V_x, V_y, V_z) = (-0.1\text{ V}, -0.1\text{ V}, -0.1\text{ V})$ for the right panel.

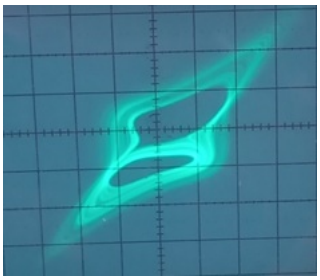

(**a**)

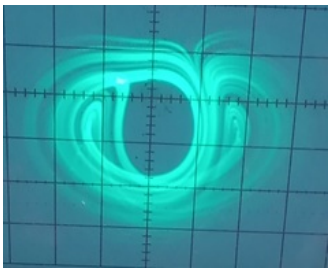

(**b**)

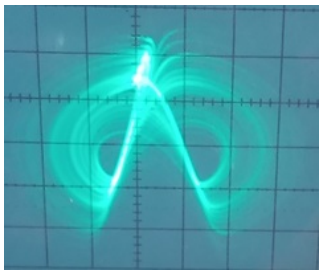

(**c**)

**Figure 9.** Captured attractors of the circuit in planes (**a**) $(V_x, V_y)$, (**b**) $(V_x, V_z)$, and (**c**) $(V_y, V_z)$.

## 4. Combination Synchronization of Oscillator

One of the successful applications of the synchronization phenomenon is in secure communication systems. Different methods have been developed for secure communications. To increase security in communication systems, some new synchronization techniques have been proposed in [41–43]. Based on the great advantages of such methods, the combination synchronization is designed. This is the combination of two drives and one response oscillator (1). The drive systems are

$$\begin{cases} \frac{dx_m}{dt} = y_m z_m \\ \frac{dy_m}{dt} = x_m^3 - y_m^3 \\ \frac{dz_m}{dt} = ax_m^2 + by_m^2 - cx_m y_m \end{cases} \tag{8}$$

where $m = 1, 2$. The response system is:

$$\begin{cases} \frac{dx_s}{dt} = y_s z_s + u_1 \\ \frac{dy_s}{dt} = x_s^3 - y_s^3 + u_2 \\ \frac{dz_s}{dt} = ax_s^2 + by_s^2 - cx_s y_s + u_3 \end{cases} \tag{9}$$

Controllers $u_i (i = 1, 2, 3)$ guarantee synchronization among the three systems. We express the error

$$e = Ax + By - Cz \tag{10}$$

where $x = (x_1, y_1, z_1)^T$, $y = (x_2, y_2, z_2)^T$, $z = (x_s, y_s, z_s)^T$, $e = (e_x, e_y, e_z)^T$ and $A$, $B$, $C \in R^{3\times3}$. The controllers $u_i$ are designed to asymptotically stabilize error (10) at the zero equilibrium. Assuming that $A = diag(\eta_1, \eta_2, \eta_3)$, $B = diag(\gamma_1, \gamma_2, \gamma_3)$ and $C = diag(\varepsilon_1, \varepsilon_2, \varepsilon_3)$, system (10) becomes

$$\begin{cases} e_x = \eta_1 x_1 + \gamma_1 x_2 - \varepsilon_1 x_s \\ e_y = \eta_2 y_1 + \gamma_2 y_2 - \varepsilon_2 y_s \\ e_z = \eta_3 z_1 + \gamma_3 z_2 - \varepsilon_3 z_s \end{cases} \tag{11}$$

The differentiation of system (11) leads to the error of dynamical system, expressed as

$$\begin{cases} \frac{de_x}{dt} = \eta_1 \frac{dx_1}{dt} + \gamma_1 \frac{dx_2}{dt} - \varepsilon_1 \frac{dx_s}{dt} \\ \frac{de_y}{dt} = \eta_2 \frac{dy_1}{dt} + \gamma_2 \frac{dy_2}{dt} - \varepsilon_2 \frac{dy_s}{dt} \\ \frac{de_z}{dt} = \eta_3 \frac{dz_1}{dt} + \gamma_3 \frac{dz_2}{dt} - \varepsilon_3 \frac{dz_s}{dt} \end{cases} \tag{12}$$

Replacing system (8), (9) and (11) into system (12) yields

$$\begin{cases} \frac{de_x}{dt} = \eta_1 y_1 z_1 + \gamma_1 y_2 z_2 - \varepsilon_1 y_s z_s - \varepsilon_1 u_1 \\ \frac{de_y}{dt} = \eta_2 (x_1^3 - y_1^3) + \gamma_2 (x_2^3 - y_2^3) - \varepsilon_2 (x_s^3 - y_s^3) - \varepsilon_2 u_2 \\ \frac{de_z}{dt} = \eta_3 (a x_1^2 + b y_1^2 - c x_1 y_1) + \gamma_3 (a x_2^2 + b y_2^2 - c x_2 y_2) - \varepsilon_3 (a x_s^2 + b y_s^2 - c x_s y_s) - \varepsilon_3 u_3 \end{cases} \tag{13}$$

From system (13), the controllers can be deduced as follows:

$$\begin{cases} u_1 = (\eta_1 y_1 z_1 + \gamma_1 y_2 z_2 - \varepsilon_1 y_s z_s - v_1)/\varepsilon_1 \\ u_2 = \left(\eta_2 (x_1^3 - y_1^3) + \gamma_2 (x_2^3 - y_2^3) - \varepsilon_2 (x_s^3 - y_s^3) - v_2\right)/\varepsilon_2 \\ u_3 = \left(\eta_3 (a x_1^2 + b y_1^2 - c x_1 y_1) + \gamma_3 (a x_2^2 + b y_2^2 - c x_2 y_2) - \varepsilon_3 (a x_s^2 + b y_s^2 - c x_s y_s) - v_3\right)/\varepsilon_3 \end{cases} \tag{14}$$

where $v_i (i = 1, 2, 3)$ are specific linear functions. Define

$$\begin{pmatrix} v_x \\ v_y \\ v_z \end{pmatrix} = \bar{A} \begin{pmatrix} e_x \\ e_y \\ e_z \end{pmatrix} \tag{15}$$

with $3 \times 3$ real matrix $\bar{A}$.

For $\bar{A} = \begin{pmatrix} -1 & 0 & 0 \\ 0 & -1 & 0 \\ -1 & -2 & -3 \end{pmatrix}$ the error dynamical system is:

$$\begin{cases} \frac{de_x}{dt} = -e_x \\ \frac{de_y}{dt} = -e_y \\ \frac{d^q e_z}{dt^q} = -e_x - 2e_y - 3e_z \end{cases} \tag{16}$$

The error dynamical system is asymptotically stable.

Numerical results (see Figure 10) verified the combination synchronization among the two drive systems (8) and the response one. Here, system (8) is chaotic for $a = 0.2$, $b = 0.1$, and $c = 0.5$. We set the initial conditions $x_1(0) = y_1(0) = z_1(0) = 0.1$, $x_2(0) = 2$, $y_2(0) = -1$, $z_2(0) = 0.1$ for two drive systems (8). The response system (9) has $x_s(0) = 1$, $y_s(0) = 0.3$, and $z_s(0) = 2$.

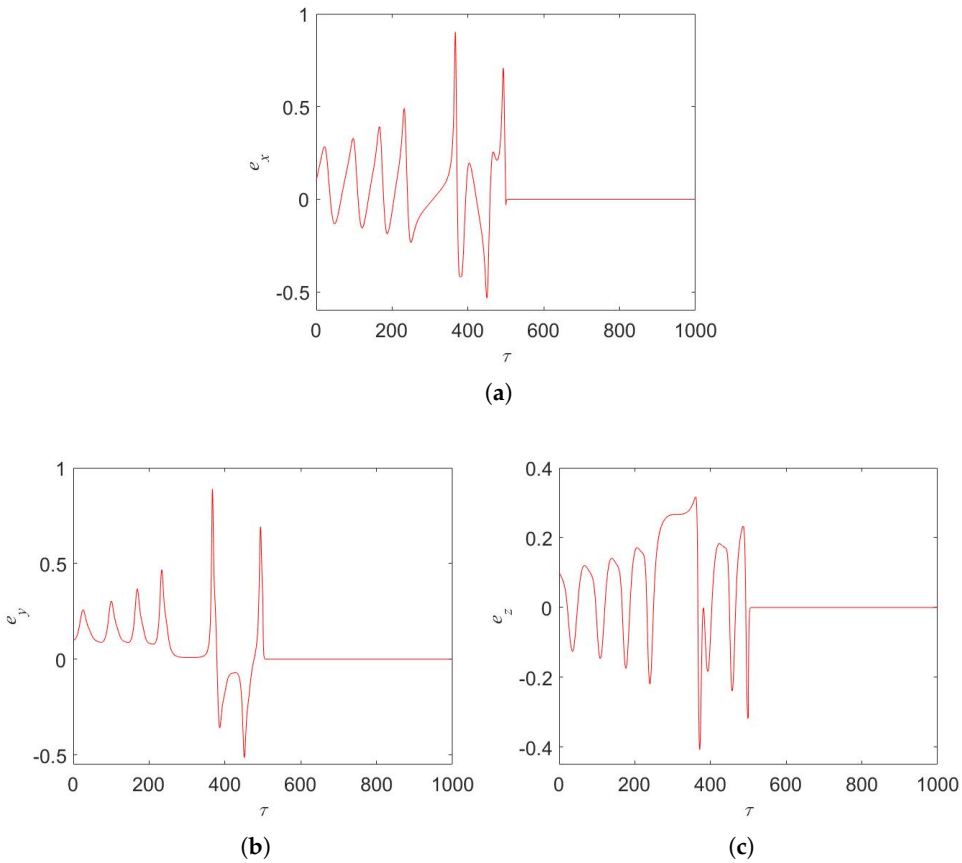


**Figure 10.** Combination synchronization errors (**a**) $e_x$, (**b**) $e_y$, (**c**) $e_z$. The control parameters are chosen as $\eta_i = \gamma_i = \varepsilon_i = 1$ $(i = 1, 2, 3)$.

## 5. Conclusions

By using nonlinear dynamic tools, we investigated an oscillator with noticeable features. The oscillator has no linear term but infinite equilibria. Chaos and symmetrical co-existing attractors were displayed by the oscillator. The results show the complex dynamics of the oscillator, which are useful for varied applications. This work contributes to special systems with different noticeable features. In our future studies, we would like to use this oscillator to generate random numbers in cryptography.

**Author Contributions:** Data curation, J.R.; Formal analysis, V.K.T.; Funding acquisition, G.G.; Investigation, V.K.T., O.A.A.; Methodology, I.H.; Project administration, G.G.; Resources, J.R.; Software, V.-T.P.; Writing—original draft, V.-T.P.; Writing—review and editing, O.A.A., I.H. All authors have read and agreed to the published version of the manuscript.

**Funding:** This work is partially funded by Centre for Nonlinear Systems, Chennai Institute of Technology, India vide funding number CIT/CNS/2021/RD/064.

**Conflicts of Interest:** The authors declare no conflict of interest.

## References

1. Wang, B.; Jahanshahi, H.; Volos, C.; Bekiros, S.; Yusuf, A.; Agarwal, P.; Aly, A.A. Control of a Symmetric Chaotic Supply Chain System Using a New Fixed-Time Super-Twisting Sliding Mode Technique Subject to Control Input Limitations. *Symmetry* **2021**, *13*, 1257. [CrossRef]
2. Wang, C.; Di, Y.; Tang, J.; Shuai, J.; Zhang, Y.; Lu, Q. The Dynamic Analysis of a Novel Reconfigurable Cubic Chaotic Map and Its Application in Finite Field. *Symmetry* **2021**, *13*, 1420. [CrossRef]
3. Wang, J.; Xiao, L.; Rajagopal, K.; Akgul, A.; Cicek, S.; Aricioglu, B. Fractional-Order Analysis of Modified Chua's Circuit System with the Smooth Degree of 3 and Its Microcontroller-Based Implementation with Analog Circuit Design. *Symmetry* **2021**, *13*, 340. [CrossRef]

4. Zang, H.; Gu, Z.; Lei, T.; Li, C.; Jafari, S. Coexisting chaotic attractors in a memristive system and their amplitude control. *Pramana* **2020**, *94*, 1–9. [CrossRef]
5. Rajagopal, K.; Bayani, A.; Jafari, S.; Karthikeyan, A.; Hussain, I. Chaotic dynamics of a fractional order glucose-insulin regulatory system. *Front. Inf. Technol. Electron. Eng.* **2020**, *21*, 1108–1118. [CrossRef]
6. Wang, S.; He, S.; Yousefpour, A.; Jahanshahi, H.; Repnik, R.; Perc, M. Chaos and complexity in a fractional-order financial system with time delays. *Chaos Solitons Fractals* **2020**, *131*, 109521. [CrossRef]
7. Moysis, L.; Tutueva, A.; Volos, C.; Butusov, D.; Munoz-Pacheco, J.M.; Nistazakis, H. A two-parameter modified logistic map and its application to random bit generation. *Symmetry* **2020**, *12*, 829. [CrossRef]
8. Panahi, S.; Shirzadian, T.; Jalili, M.; Jafari, S. A new chaotic network model for epilepsy. *Appl. Math. Comput.* **2020**, *346*, 395–407. [CrossRef]
9. Parastesh, F.; Aram, Z.; Namazi, H.; Sprott, J.C.; Jafari, S. A simple chaotic model for development of HIV virus. *Sci. Iran.* **2021**, *28*, 1643–1652.
10. Chen, X.; Qian, S.; Yu, F. Pseudorandom Number Generator Based on Three Kinds of Four-Wing Memristive Hyperchaotic System and Its Application in Image Encryption. *Complexity* **2020**, *2020*, 8274685. [CrossRef]
11. Yu, F.; Shen, H.; Zhang, Z.; Huang, Y.; Cai, S.; Du, S. Dynamics analysis, hardware implementation and engineering applications of novel multi-style attractors in a neural network under electromagnetic radiation. *Chaos Solitons Fractals* **2021**, *152*, 111350. [CrossRef]
12. Garcia-Guerrero, E.E.; Inzunza-Gonzalez, E.; Lopez-Bonilla, O.R.; Cardenas-Valdez, J.R.; Cuautle, E.T. Randomness improvement of chaotic maps for image encryption in a wireless communication scheme using PIC-microcontroller via Zigbee channels. *Chaos Solitons Fractals* **2020**, *133*, 109646. [CrossRef]
13. Petavratzis, E.; Moysis, L.; Volos, C.; Stouboulos, I.; Nistazakis, H.; Valavanis, K. A chaotic path planning generator enhanced by a memory technique. *Rob. Auton. Syst.* **2021**, *143*, 103826. [CrossRef]
14. la Fraga, L.G.D.; Mancillas-Lopez, C.; Tlelo-Cuautle, E. Designing an authenticated Hash function with a 2D chaotic map. *Nonlinear Dyn.* **2021**, *104*, 4569–4580. [CrossRef]
15. Mobayen, S.; Volos, C.; Cavusoglu, U.; Kacar, S.S. A Simple Chaotic Flow with Hyperbolic Sinusoidal Function and Its Application to Voice Encryption. *Symmetry* **2020**, *12*, 2047. [CrossRef]
16. Adeyemi, V.A.; Nunez-Perez, J.C.; Ibarra, Y.S.; Perez-Pinal, F.J.; Tlelo-Cuautle, E. FPGA Realization of the Parameter-Switching Method in the Chen Oscillator and Application in Image Transmission. *Symmetry* **2021**, *13*, 923. [CrossRef]
17. Muhammad, A.S.; Ozkaynak, F. SIEA: Secure Image Encryption Algorithm Based on Chaotic Systems Optimization Algorithms and PUFs. *Symmetry* **2021**, *13*, 824. [CrossRef]
18. Yu, F.; Shen, H.; Zhang, Z.; Huang, Y.; Cai, S.; Du, S. A new multi-scroll Chua's circuit with composite hyperbolic tangent-cubic nonlinearity: Complex dynamics, Hardware implementation and Image encryption application. *Integration* **2021**, *81*, 71–83. [CrossRef]
19. Yu, F.; Li, L.; He, B.; Liu, L.; Qian, S.; Zhang, Z.; Shen, H.; Cai, S.; Li, Y. Pseudorandom number generator based on a 5D hyperchaotic four-wing memristive system and its FPGA implementation. *Eur. Phys. J. Spec. Top.* **2021**, *230*, 1763–1772. [CrossRef]
20. Yu, F.; Zhang, Z.; Shen, H.; Huang, Y.; Cai, S.; Jin, J.; Du, S. Design and FPGA implementation of a pseudo-random number generator based on a Hopfield neural network under electromagnetic radiation. *Front. Phys.* **2021**, *9*, 690651. [CrossRef]
21. Tutueva, A.V.; Karimov, T.I.; Moysis, L.; Nepomuceno, E.G.; Volos, C.; Butusov, D.N. Improving chaos-based pseudo-random generators in finite-precision arithmetic. *Nonlinear Dyn.* **2021**, *105*, 727–737. [CrossRef]
22. Sajad, S.; Kapitaniak, T. Special chaotic systems. *Eur. Phys. J. Spec. Top.* **2020**, *229*, 877–886.
23. Xu, Y.; Yang, Y. A new chaotic system without linear term and its impulsive synchronization. *Optik* **2014**, *125*, 2526–2530. [CrossRef]
24. Mobayen, S.; Kingni, S.; Pham, V.T.; Nazarimehr, F.; Jafari, S. Analysis, synchronisation and circuit design of a new highly nonlinear chaotic system. *Int. J. Syst. Sci.* **2018**, *49*, 617–630. [CrossRef]
25. Zhang, S.; Zeng, Y.; Li, Z. Chaos in a novel fractional order system without a linear term. *Int. J. Nonlinear Mech.* **2018**, *106*, 1–12. [CrossRef]
26. Khalil, H. *Nonlinear Systems*; Prentice Hall: Englewood Cliffs, NJ, USA, 2002.
27. Sprott, J.C. *Elegant Chaos: Algebraically Simple Chaotic Flows*; World Scientific: Singapore, 2010.
28. Wang, X.; Chen, G. Constructing a chaotic system with any number of equilibria. *Nonlinear Dyn.* **2013**, *71*, 429–436. [CrossRef]
29. Leonov, G.A.; Kuznetsov, N.V. Hidden attractors in dynamical systems: From hidden oscillation in Hilbert-Kolmogorov, Aizerman and Kalman problems to hidden chaotic attractor in Chua circuits. *Int. J. Bif. Chaos* **2013**, *23*, 1330002. [CrossRef]
30. Jafari, S.; Sprott, J.C. Simple chaotic flows with a line equilibrium. *Chaos Solitons Fractals* **2013**, *57*, 79–84. [CrossRef]
31. Wang, Z.; Wei, Z.; Sun, K.; Shaobo He, H.W.; Xu, Q.; Chen, M. Chaotic flows with special equilibria. *Eur. Phys. J. Spec. Top.* **2020**, *229*, 905–919. [CrossRef]
32. Hens, C.; Dana, S.K.; Feudel, U. Extreme multistability: Attractors manipulation and robustness. *Chaos* **2015**, *25*, 053112. [CrossRef]
33. Bao, B.; Qian, H.; Xu, Q.; Chen, M.; Wang, J.; Yu, Y. Coexisting Behaviors of Asymmetric Attractors in Hyperbolic-Type Memristor based Hopfield Neural Network. *Front. Comput. Neurosci.* **2017**, *11*, 81. [CrossRef]
34. Li, C.; Sun, J.; Lu, T.; Lei, T. Symmetry Evolution in Chaotic System. *Symmetry* **2020**, *12*, 574. [CrossRef]

35. Thoai, V.P.; Kahkeshi, M.S.; Huynh, V.V.; Ouannas, A.; Pham, V.T. A Nonlinear Five-Term System: Symmetry, Chaos, and Prediction. *Symmetry* **2020**, *12*, 865. [CrossRef]
36. Xu, Q.; Lin, Y.; Bao, B.; Chen, M. Multiple attractors in a non-ideal active voltage- controlled memristor based Chua's circuit. *Chaos Solitons Fractals* **2016**, *83*, 186–200. [CrossRef]
37. Xu, Q.; Cheng, S.; Ju, Z.; Chen, M.; Wu, H. Asymmetric coexisting bifurcations and multi-stability in an asymmetric memristive diode-bridge-based jerk circuit. *Chin. J. Phys.* **2021**, *70*, 69–81. [CrossRef]
38. Wolf, A.; Swift, J.B.; Swinney, H.L.; Vastano, J.A. Determining Lyapunov exponents from a time series. *Physica D* **1985**, *16*, 285–317. [CrossRef]
39. Li, C.; Sprott, J.C. Variable-boostable chaotic fows. *Opt. Int. J. Light Electron Opt.* **2016**, *27*, 10389–10398. [CrossRef]
40. Tamba, V.K.; Karthikeyan, R.; Pham, V.T.; Hoang, D.V. Chaos in a system with an absolute nonlinearity and chaos synchronization. *Opt. Int. J. Light Electron Opt.* **2018**, *2018*, 5985489. [CrossRef]
41. Feng, C.F.; Tan, Y.R.; Wang, Y.H.; Yang, H.J. Active backstepping control of combined projective synchronization among different nonlinear systems. *Automatika* **2018**, *58*, 295–301. [CrossRef]
42. Runzi, L.; Yinglan, W.; Shucheng, D. Combination synchronization of three classic chaotic systems using active backstepping design. *Chaos* **2012**, *22*, 023109. [CrossRef]
43. Pone, J.R.M.; Kingni, S.T.; Kol, G.R.; Pham, V.T. Hopf bifurcation, antimonotonicity and amplitude controls in the chaotic Toda jerk oscillator: Analysis, circuit realization and combination synchronization in its fractional-order form. *Automatika* **2019**, *60*, 149–161. [CrossRef]